Colloid Polym Sci (2008) 286:469–473
DOI 10.1007/s00396-007-1812-8

SHORT COMMUNICATION

Eu(III)-modified properties of thermosensitive core–shell microspheres

Xiaoyun Guo · Tianhong Lu · Xiaohua Huang

Received: 14 October 2007 / Revised: 21 November 2007 / Accepted: 24 November 2007 / Published online: 8 January 2008

Abstract We successfully prepared PNIPAM-g-P(NIPAM-co-St) (PNNS) core–shell microsphere by an emulsifier-free emulsion polymerization method. When PNNS with a core–shell structure is interacted with Eu(III), Eu(III) mainly bonds to oxygen of the carbonyl groups of PNNS, forming the novel PNNS-Eu(III) complex. It was found that the complex showed thermosensitive and fluorescent properties at one time. Especially, the maximum emission intensity of Eu(III) in the complex at 614 nm is significantly enhanced in comparison with that of pure Eu(III), demonstrating that there exists an efficient intermolecular energy transfer from the polymer ligand to Eu(III) and then the excited Eu(III) generates the enhanced fluorescence. When the weight ratio of Eu(III) and the PNNS is 8 wt%, the enhancement of the emission fluorescence intensity at 614 nm is highest.

Keywords Microsphere · Europium · Thermosensitive · Luminescence

Introduction

Until now, the potential applications of poly(*N*-isopropylacrylamide) (PNIPAM) materials have been under intensive study in recent years as a result of their potential uses in numerous fields such as controlled drug delivery, biosensors, bioseparation, catalysis, and magnetically controlled electrochemical reactions [1–5] because its lower critical solution temperature (LCST, approximately 32 °C) [6] is very close to the physiologic temperature. For the potential applications of these microspheres, further functionalization of them is needed. To improve the biocompatibility of this material, Akashi et al. [7, 8] grafted other materials with better hydrophilicity onto the PNIPAM backbone and acquired novel materials with better biocompatibility.

In our previous work [9], when Tb(III) was interacted with linear PNIPAM and formed the PNIPAM-Tb(III) complex, it was found that the complex became more intelligent. However, the linear PNIPAM exists as the random coil and has bad repeatability. It is well known that the nanomaterials exhibit novel properties compared with the bulk materials. So we prepared the PNIPAM-g-P(NIPAM-co-St) (PNNS) microsphere by an emulsifier-free emulsion polymerization method. Meanwhile, we chose Eu(III) to coordinate with PNNS and hoped that a new material with high intelligence and better quality could be obtained.

Experimental

NIPAM (Aldrich Chemical; 99%) was used without further purification. Styrene (St) was distilled under reduced pressure and then stored in the refrigerator before use. $EuCl_3$ was prepared according to the method described in the literature [10]. Other reagents were of analytical grade.

PNNS was synthesized according to the method described in the literature [11]. Nine grams St and 1 g NIPAM were dissolved in 175 ml deionized water in a 250-ml four-necked round-bottom flask equipped with a condenser, a nitrogen inlet, a thermometer, and a stirrer. Nitrogen was bubbled into the solution, and the mixture was stirred for 30 min to remove oxygen from the solution. Polymerization

X. Guo · T. Lu · X. Huang (✉)
Jiangsu Key Laboratory of Biofunctional Material,
College of Chemistry and Environmental Science,
Nanjing Normal University,
Nanjing 210097, People's Republic of China
e-mail: wxxhhuang@yahoo.com

was initiated by adding 15 ml of aqueous solution containing a certain amount of $K_2S_2O_8$ at 70 °C. The reaction was allowed to proceed for 24 h at 70 °C under stirring. The resulting P(NIPAM-co-St) samples were dialyzed and purified by repetitive centrifugation, decantation, and redispersion and then freeze-dried. Then, the PNIPAM shell layers were prepared using the above-prepared P(NIPAM-co-St) core as the seeds by a seed polymerization method. One gram NIPAM, 0.1 g and 0.01 g $K_2S_2O_8$ was dissolved in 15 ml deionized water and then added into the above-prepared P(NIPAM-co-St) suspension. After 12 h under intermittent microwave irradiation, the product was obtained. After the product was dialyzed and purified by repetitive centrifugation, decantation, and redispersion, it was freeze-dried. The preparation procedure of the PNNS-Eu(III) complex is as follows: For preparing the PNNS-Eu(III) complex with the weight ratio of Eu^{3+}/PNNS=0.08:1, 0.136 g $EuCl_3$ and 1 g PNNS were dissolved in ethanol. The mixture solution was stirred for 24 h at 25 °C. The product was purified and then dried in the vacuum at room temperature for 48 h. Finally, the PNNS-Eu(III) complex was obtained. For preparing the PNNS-Eu(III) complexes with other weight ratios, the weights of $EuCl_3$ and PNNS were changed to the corresponding values.

The TEM micrographs of the samples were obtained using a Hitachi (H-7000, Japan) transmission electron microscope at a 75-kV accelerating voltage. The TEM samples were prepared with placing a drop of a highly diluted suspension of the sample in a 400-mesh carbon-coated copper grid and subsequently dried. The XPS spectra (Mg Ka) were recorded with a VG Scientific ESCALAB. The particle size of the nanoparticles was determined using a dynamic laser scattering particle sizer (ALV-5000, German) at 25 °C. A German Perkin-Elmer model Ls50B fluorescence spectrophotometer was used to measure the fluorescence spectra of PNNS and PNNS-Eu(III).

Results and discussion

TEM measurement

It can be clearly observed from Fig. 1a and b that the particles of PNNS and the PNNS-Eu(III) complex possess the core–shell structure because the density of the core is different from that of the shell [12]. The average particle sizes of PNNS and the PNNS-Eu(III) complex are 112 and 120 nm, respectively. It illustrated that after Eu(III) forms the complex with PNNS, the thickness of the shell is increased by about 5 nm. Thus, it can be deduced that Eu (III) may be interacted with the acylamino groups in PNNS, a strong electrostatic repulsion between core and shell

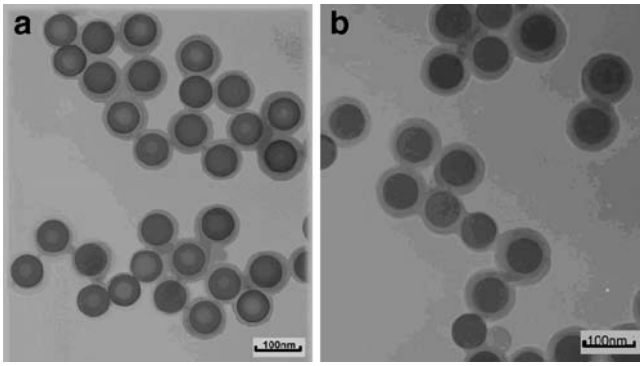

Fig. 1 The TEM images of **a** PNNS and **b** the PNNS-Eu(III) complex with the weight ratio of 0.08:1

generated by Eu(III) results in a certain swelling of PNNS [13].

Formation mechanism of the PNNS-Eu(III) complex

XPS measurement has become a powerful tool for providing precise information concerning the core-level binding energies and the valence electronic structure of macromolecules [14]. The XPS spectra of PNNS and the PNNS-Eu(III) complex are shown in Fig. 2. The average binding energy values of C_{1s}, O_{1s}, N_{1s}, and Eu_{4d} of PNNS and the PNNS-Eu(III) complex are listed in Table 1. It was reported that the binding energy of N_{1s} for the C–N bonds is at about 400 eV and the binding energy of O_{1s} for the C–O bonds is at about 531 eV [15]. Thus, the average binding energies of O_{1s} and N_{1s} in Table 1 are mainly contributed from the C–O and C–N bonds in PNNS and the PNNS-Eu(III) complex. It was clearly observed from Table 1 that the average binding energies of N_{1s} and O_{1s} of the PNNS-Eu(III) complex were increased by about 0.31 and 1.12 eV, respectively, comparing with that of PNNS,

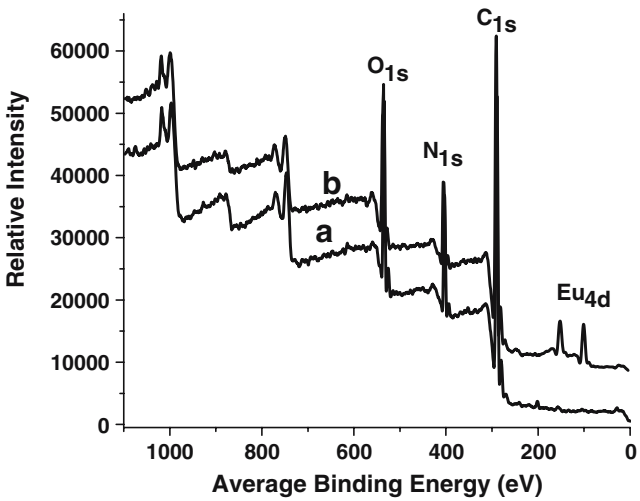

Fig. 2 The XPS spectra of *a* PNNS and *b* the PNNS-Eu(III) complex with the weight ratio of 0.08:1

Table 1 The binding energies of C_{1s}, O_{1s}, N_{1s}, and Eu($4d_{5/2}$) for PNNS and the PNNS-Eu(III) complex

Condition	C_{1s} (eV)	O_{1s} (eV)	N_{1s} (eV)	Eu($4d_{5/2}$) (eV)
PNNS	284.6	529.29	400.41	–
PNNS-Eu(III)	284.6	530.41	400.72	136.68
$EuCl_3$	–	–	–	141.21

leading to the decrease in the electron density of the N_{1s} and O_{1s} atoms in the PNNS-Eu(III) complex. Meanwhile, the average binding energy of Eu($4d_{5/2}$) was decreased by about 4.53 eV, leading to the increase in the electron density of Eu(III) in the PNNS-Eu(III) complex. Therefore, the results from the experiment mentioned above further demonstrated that the PNNS-Eu(III) complexes may be formed with the coordination between Eu(III) and O of the carbonyl group [16]. After the electron density of O is decreased due to the coordination with Eu(III), the electron cloud of N would be shifted to O due to the inducement effects, leading to the decrease in the electron density of N and increase in the average binding energy of N [17].

LCST measurement

As shown in Fig. 3, the R_h of PNNS (curve a) and PNNS-Eu(III) (curve b) changed with the temperature because the PNIPAM chains can absorb or lose water at the temperature lower or higher than LCST, and thus, it would undergo a volume transition with the temperature in the aqueous solution. LCST was defined as the onset temperature of the endotherm [18]. It can be found that the LCST of the PNNS-Eu(III) complex is slightly higher than that of PNNS because the coordination between Eu(III) and PNNS increases the rigid planar structure of PNNS [19]. It also illustrated that the PNNS-Eu(III) complex with low content of Eu(III) does not largely change the temperature-responsive property of PNNS [20].

Fluorescence characterization

The excitation fluorescence spectra of $EuCl_3$, PNNS, and the PNNS-Eu(III) complex are shown in Fig. 4. In the excitation spectrum of $EuCl_3$ (Fig. 4, curve a), only the negligible excitation peaks were observed. For PNNS, the main peak is located at 250 nm (Fig. 4, curve b). However, PNNS-Eu(III) complexes show a different spectral shape and stronger absorption intensity compared with that of PNNS in the range of 220–300 nm attributed to the $\pi \rightarrow \pi^*$ transition by exciting the carbonyl group of PNNS-Eu(III). For these significant phenomena, the only reasonable explanation is the formation of the PNNS-Eu(III) complexes. This may lead to electronic delocalization and may strongly absorb ultraviolet light. Therefore, it greatly enhanced the absorption intensity.

The emission fluorescence spectra were obtained under excitation at 270 nm (which was selected from the excitation spectrum of the PNNS-Eu(III) complex). It can be observed from Fig. 5, curve a that the characteristic emission fluorescence peaks of Eu(III) are very weak. In Fig. 5, curve b, the strong peaks around 305 nm are assigned to the emission peaks of PNNS. The maximum emission intensity of the PNNS nanoparticle at 305 nm is enhanced about 1.7 times, compared with that of the corresponding peak of linear PNIPAM [9]. In Fig. 5, curve c, except for the emission peaks around 305 nm, three narrow and strong characteristic emission peaks at 580, 592, and 614 nm were observed. They are corresponded to the $^5D_0 \rightarrow {}^7F_0$, $^5D_0 \rightarrow {}^7F_1$, $^5D_0 \rightarrow {}^7F_2$ electronic transition of Eu(III). The strongest peak is located at 614 nm

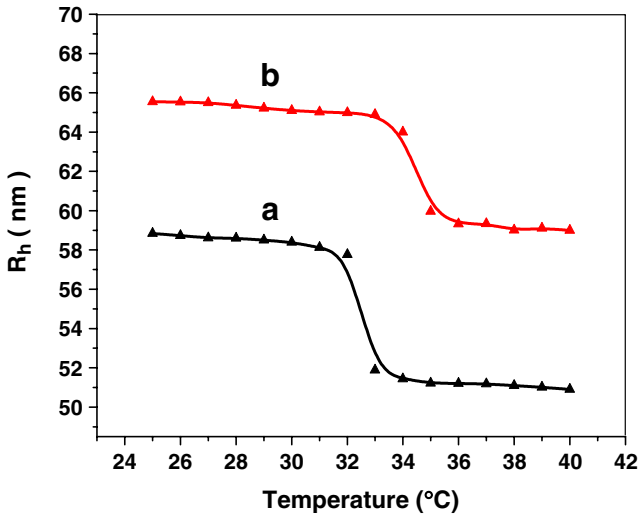

Fig. 3 The relationship of the temperature and R_h of *a* PNNS and *b* the PNNS-Eu (III) complex with the weight ratio of 0.08:1

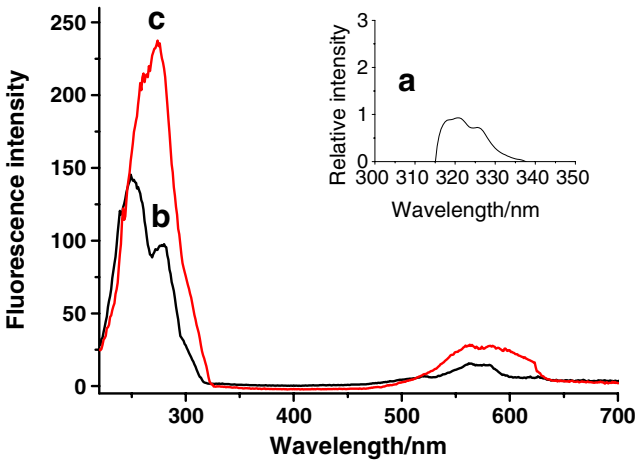

Fig. 4 The excitation fluorescence spectra of *a* $EuCl_3$, *b* PNNS, and *c* the PNNS-Eu(III) complex with the weight ratio of 0.08:1. Emission wavelength=614 nm (split width=5/5)

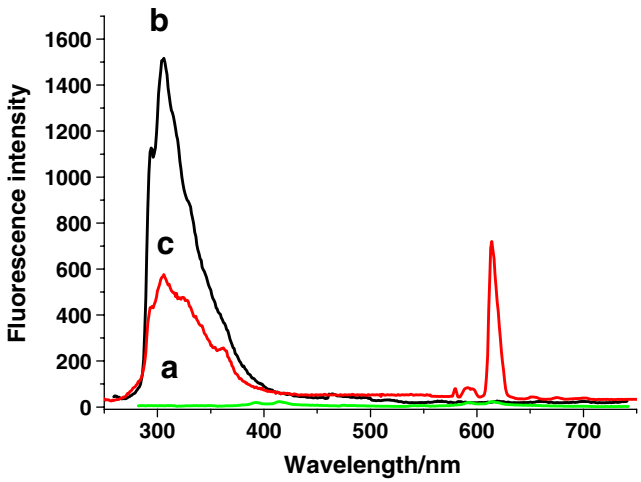

Fig. 5 The emission fluorescence spectra of *a* $EuCl_3$, *b* PNNS, and *c* the PNNS-Eu(III) complex with the weight ratio of 0.08:1. Excitation wavelength=270 nm (split width=5/5)

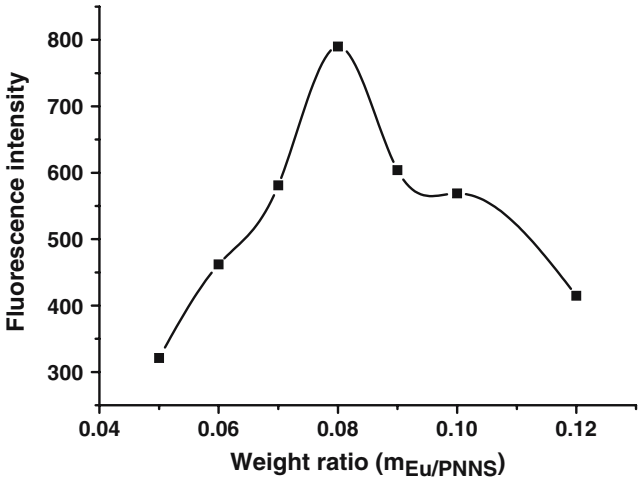

Fig. 6 The plot of the intensity of the emission peak of the PNNS-Eu(III) complex at 614 nm vs the weight ratio of Eu(III) (split width=5/5)

($^5D_0 \rightarrow ^7F_2$). Owing to the shielding of the 4*f* orbital by an outer shell of the 5*s* and 5*p* orbital, the *f*–*f* absorption bands of Eu(III) are very narrow [21]. This transition is responsible for the red color emitted by the complex. The maximum emission intensity of the PNNS-Eu(III) complex at 614 nm is enhanced about 33 times compared with that of the corresponding peak of $EuCl_3$ (Fig. 5, curve a). According to the energy transferring mechanism of complexes [22], the intramolecular energy transfer efficiency from the organic ligands to Eu(III) is the most important factor for influencing the luminescent properties of the Eu (III) complexes. If the triplet energy is low, backtransfer from Eu(III) to the ligand occurs. The absorption coefficient of Eu(III) is small at the ultraviolet region, while the PNNS-Eu(III) complex has a strong absorption in the ultraviolet range and emits strong green luminescence. The intramolecular energy transfer efficiency reaches 55%, which was obtained according to the ratio of the peak areas [23], suggesting that PNNS transfers its energy to Eu(III) after absorbing the photon energy, and then the excited Eu(III) generates the enhanced fluorescence [24]. It means that the energy level of the triplet state of Eu(III) approaches to PNNS, and the energy level of PNNS is suitable for transferring energy to Eu(III). In addition, the decrease in loss of transferring energy with the orderly conformation may be another reason of the enhancement of the emission fluorescence intensity at 614 nm.

Figure 6 shows the relationship between the $^5D_0 \rightarrow ^7F_2$ fluorescence emission intensity of Eu(III) at 614 nm and the weight ratio of Eu(III) and PNNS. It can be clearly observed from Fig. 6 that the emission fluorescence intensity of the $^5D_0 \rightarrow ^7F_2$ transition of Eu(III) at 614 nm is related to the weight ratio of Eu(III) and PNNS. The intensity increases with increasing weight ratio until the weight ratio reaches 8 wt%, and decreases with the further increase in the content of Eu(III). It is because when the weight ratio is too high, Eu(III) ions are close enough to produce the nonradiative energy transfer from the triplet state to the single ground state, leading to the decrease in the probability of the $^5D_0 \rightarrow ^7F_2$ transition [25].

Figure 7 shows the relationship between the temperature and the emission intensity of the peak at 614 nm of the PNNS-Eu(III) complex. It can be seen in Fig. 7 that when the temperature is lower than 33 °C, the emission intensity changes a little bit with increasing temperature for the PNNS-Eu(III) complex. When the temperature is higher than 33 °C, the emission intensity increases significantly with increasing temperature. The above result is related to the change in the structure of the PNNS-Eu(III) complex with the temperature. When the temperature is below 33 °C, the PNNS-Eu(III) complex exists as a hydrophilic coil and is water-soluble. Their conformation is not changed with a

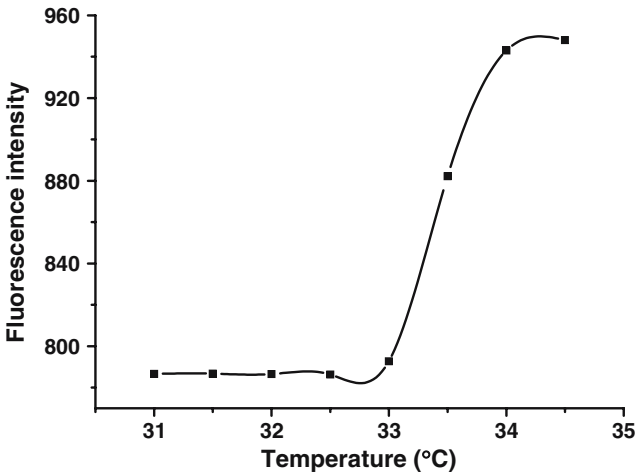

Fig. 7 The relationship between the temperature and the emission intensity of the peak at 614 nm of the PNNS-Eu(III) complex with the weight ratio of 0.08:1 (split width=5/5)

temperature below 33 °C. Thus, the emission intensity is almost the same at a temperature below 33 °C However, when the temperature increases, the emission intensity increases with increasing temperature because the conformation of the PNNS-Eu(III) complex changes from the hydrophilic coil to the hydrophobic globule and then the water-soluble PNNS-Eu (III) complex becomes water insoluble.

Conclusions

From the above experimental results, it could be concluded that when PNNS is interacted with Eu(III), Eu(III) mainly bonded to O of the carbonyl group of PNNS, forming the novel PNNS-Eu(III) complexes. The complex possesses not only the characteristic fluorescence of Eu(III), but also the temperature responsive property of PNNS. Especially, the emission fluorescence intensity of Eu(III) in the complex at 614 nm is significantly enhanced. When the weight ratio of Eu(III) and the PNNS is 8 wt%, the enhancement of the emission fluorescence intensity at 614 nm is highest.

Acknowledgments The authors are grateful for the financial support of the National Natural Science Foundation of China (No. 20471030) and the Science and Technology Project from Jiangsu province (BG2005040).

References

1. Kim EJ, Cho SH, Yuk SH (2001) Biomaterials 22:2495
2. Zhu L, Zhu G, Li M, Wang E, Zhu R, Qi X (2002) Eur Polym J 38:2503
3. Kawaguchi H, Fujimoto K (1998) Bioseparation 7:253
4. Jones CD, Lyon LA (2000) Macromolecules 3:8301
5. Katz E, Baron R, Willner I (2005) J Am Chem Soc 127:4060
6. Gao J, Wu C (1997) Macromolecles 30:6873
7. Hsiue GH, Chang RW, Wang CH, Lee SH (2003) Biomaterials 24:2423
8. Kaneko T, Asoh T, Fukushige Y, Akashi M (2006) Macromolecules 9:2298
9. Yin WQ, Chen MQ, Lu TH, Akashi M, Huang XH (2006) Eur Polym J 42:1305
10. Taylor MD, Carter CP (1962) J Inorg Nucl Chem 24:387
11. Nakahama K, Fujimoto K (2002) Langmuir 18:10095
12. Lei L, Gohy JF, Willet N, Zhang JX, Varshney S, Jerome R (2004) Macromolecules 37:1089
13. Goodman D, Kizhakkedathu JN, Brooks DE (2004) Langmuir 20:2333
14. Beamson G, Briggs D (1992) High resolution XPS of organic polymers. Wiley, New York
15. Sabbatini L, Malitesta C, De Giglio E, Losito I, Torsi L, Zambonin PG (1999) J Electron Spectrosc Relat Phenom 100:35
16. Drolet DP, Manuta DM, Lees AJ, Katnani AD, Coyle GJ (1988) Inorg Chim Acta 146:173
17. Xu J, Huang XH, Zhou NL, Zhang JS, Bao JC, Lu TH et al (2004) Mater Lett 58:1938
18. Otake K, Inomata H, Konno M, Saito S (1990) Macromolecules 23:283
19. Tanaka T, Fillmore D, Sun ST, Nishio I, Gerald S, Arati S (1980) Phys Rev Lett 45:1636
20. Suetoh Y, Shibayama M (2000) Polymer 41:505
21. Li Q, Li T, Wu JG (2001) J Phys Chem B 105:12293
22. Lakowicz JR (1983) Principles of fluorescence spectroscopy. Plenum, New York
23. Nagata I, Li R, Banks E, Okamoto Y (1983) Macromolecules 16:903
24. Okamoto Y, Ueba Y, Nagata I, Banks E (1981) Macromolecules 14:807
25. Okamoto Y, Ueba Y, Dzhanibekov NF, Banks E (1981) Macromolecules 14:17